

## PHYSICS CONTRIBUTION

## INCLUSION OF GEOMETRICAL UNCERTAINTIES IN RADIOTHERAPY TREATMENT PLANNING BY MEANS OF COVERAGE PROBABILITY

JOEP C. STROOM, M.Sc.,\* HANS C. J. DE BOER, M.Sc.,\* HENK HUIZENGA, Ph.D.,<sup>†</sup> AND  
ANDRIES G. VISSER, Ph.D.\*

\*University Hospital Rotterdam, Daniel den Hoed Cancer Center, Department of Clinical Physics, Rotterdam, The Netherlands; and

<sup>†</sup>University of Nijmegen, Institute of Radiotherapy, Nijmegen, The Netherlands

**Purpose:** Following the ICRU-50 recommendations, geometrical uncertainties in tumor position during radiotherapy treatments are generally included in the treatment planning by adding a margin to the clinical target volume (CTV) to yield the planning target volume (PTV). We have developed a method for automatic calculation of this margin.

**Methods and Materials:** Geometrical uncertainties of a specific patient group can normally be characterized by the standard deviation of the distribution of systematic deviations in the patient group ( $\Sigma$ ) and by the average standard deviation of the distribution of random deviations ( $\sigma$ ). The CTV of a patient to be planned can be represented in a 3D matrix in the treatment room coordinate system with voxel values one inside and zero outside the CTV. Convolution of this matrix with the appropriate probability distributions for translations and rotations yields a matrix with coverage probabilities (CPs) which is defined as the probability for each point to be covered by the CTV. The PTV can then be chosen as a volume corresponding to a certain iso-probability level. Separate calculations are performed for systematic and random deviations. Iso-probability volumes are selected in such a way that a high percentage of the CTV volume (on average > 99%) receives a high dose (> 95%). The consequences of systematic deviations on the dose distribution in the CTV can be estimated by calculation of dose histograms of the CP matrix for systematic deviations, resulting in a so-called dose probability histogram (DPH). A DPH represents the average dose volume histogram (DVH) for all systematic deviations in the patient group. The consequences of random deviations can be calculated by convolution of the dose distribution with the probability distributions for random deviations. Using the convolved dose matrix in the DPH calculation yields full information about the influence of geometrical uncertainties on the dose in the CTV.

**Results:** The model is demonstrated to be fast and accurate for a prostate, cervix, and lung cancer case. A CTV-to-PTV margin size which ensures at least 95% dose to (on average) 99% of the CTV, appears to be equal to about  $2\Sigma + 0.7\sigma$  for three all cases. Because rotational deviations are included, the resulting margins can be anisotropic, as shown for the prostate cancer case.

**Conclusion:** A method has been developed for calculation of CTV-to-PTV margins based on the assumption that the CTV should be adequately irradiated with a high probability. © 1999 Elsevier Science Inc.

PTV margin, Organ motion, Setup deviation, Coverage probability, Conformal therapy.

## INTRODUCTION

Geometrical uncertainties in radiotherapy treatments cause differences between intended and actually delivered dose distribution in the clinical target volume (CTV), as defined by the International Commission on Radiation Units and Measurements (ICRU) (1). The uncertainties primarily consist of external setup deviations and internal organ movement. Both deviations consist of a systematic component, i.e., the same for each fraction of the treatment, as well as a random component, i.e., varying from day to day. The size of the patient setup deviations can be assessed by compar-

ison of images acquired during the treatment (with megavoltage portal films or electronic portal imaging devices) with those of the intended treatment (simulator radiographs or digitally reconstructed radiographs generated by the planning system). By imaging several patients of a specific patient group regularly, the typical size of the systematic and the random positioning deviations for that group can be determined (2, 3), which may indirectly lead to improved setup techniques and/or equipment. In principle, systematic deviations of an individual patient can be estimated during the first few fractions and couch corrections can be applied

Supported by a grant of the Dutch Cancer Society.

Reprint requests to: J.C. Stroom, University Hospital Rotterdam, Daniel den Hoed Cancer Center, Department of Clinical Physics, Groene Hilledijk 301, 3075 EA Rotterdam, The Netherlands.

**Acknowledgments**—The authors thank the Dutch Cancer Society

for their financial support (project MVA2 92-86). The discussions with Erik van Dieren, Ben Heijmen, and Arjan Bel have been a great help during the development of the model and the writing of the paper. The aid of John van Sörnsen de Koste, Gert Korevaar, and Sandra Quint with the computer planning was much appreciated.

Accepted for publication 29 October 1998.

for subsequent irradiations (4–6). This so-called “off-line protocol” reduces systematic deviations while random deviations remain unchanged. Both systematic and random setup deviations can be reduced to negligible values if on-line corrections are applied (7, 8). In this case, the patient position is verified at each fraction using a small number of monitor units. If necessary, the couch position is adjusted before the remaining dose is given. At the moment, however, on-line correction procedures are too time-consuming to be routinely used in clinical practice.

Internal organ motion is the movement of an organ relative to the bony structures. For instance, the prostate can move due to variations in bladder and rectum filling. These movements can not be assessed directly by portal imaging since the tumor is generally not visible. By implantation of radiopaque markers in or near the CTV the internal organ motion can be visualized which enables on-line positioning corrections (9, 10). In other clinical studies repeated computed tomographic (CT) scans have been acquired to get an indication of internal prostate movements (11, 12). Intrafraction movement of the tumor will add to the random deviation. Due to breathing and cardiac motion, a tumor in thorax or abdomen can vary significantly in position in a matter of seconds (13). Complex techniques like real-time couch movement, respiration gated irradiation, or breathing control might limit the consequences of this variation (14–16).

Whatever is done to minimize the geometrical uncertainties, to some extent inaccuracies are unavoidable. Once the typical values for a specific group of patients are known, they should be included in the treatment planning for individual patients from that group. Patient setup deviations not only affect the dose in the tumor region, but in neighboring, possibly critical, organs as well. For random deviations, the effect of this deviation can be simulated by a convolution of the dose distributions with the distribution of movements in three dimensions. Several groups have implemented this for translational deviations (17, 18). Systematic deviations are more of a problem since they are *a priori* not known for a specific patient and only the distribution of systematic deviations for the patient group can be determined. The effect of systematic deviations on the dose distribution is more significant than that of random deviations, hence relatively small systematic deviations should not be ignored. One possible way to deal with systematic deviations has been proposed by Goitein (19). He suggested three parallel planning calculations, one with nominal setup deviations and the others with extreme values, and allow only those plans for which all three dose distributions are acceptable in terms of tumor coverage and critical organ sparing. Recently this idea has been further developed by Mageras and colleagues, especially to include internal organ motion in radiotherapy planning (20). Killoran and colleagues simulate systematic and random uncertainties simultaneously by multiple Monte Carlo simulations which result in multiple dose volume histograms (DVHs) that are used for evaluation of the treatment plan (21).

The above techniques operate directly on the CTV and

are more sophisticated than the conventional approach as proposed by the ICRU (1), i.e., using a planning target volume (PTV) which is defined as the CTV plus margins for all geometrical uncertainties. However, the practical application of the concept of PTV is not always clear. First, it is rather cumbersome to manually draw margins in three dimensions around an irregularly shaped tumor volume (22). Therefore several groups have developed algorithms for automatic margin calculation, either multiple 2D (23) or fully 3D (24, 25). Furthermore, the geometrical uncertainties can originate from rotations as well as translations. Rotational deviations will yield anisotropic margins, i.e., the size of the margin will vary depending on the position with respect to the axis of rotation. None of the aforementioned algorithms have incorporated this. Finally, the exact margin size necessary to ascertain adequate coverage of the CTV depends on the kind of deviation (systematic or random) and on the dose distribution. How this must be taken into account has up till now not been specified.

We have developed a model that calculates the CTV-to-PTV margins step by step, based on clinically measured CTV position deviations and on the requirement that the dose distribution delivered to the CTV will satisfy the ICRU recommendations for dose homogeneity with a high probability. Internal organ motion as well as external setup deviations, translations as well as rotations, and systematic as well as random deviations are included in the model. Once the dose distribution has been planned around the resulting PTV, the same algorithms can be used to calculate the influence of all geometrical uncertainties on the dose in the CTV and hence to verify the planned dose distribution. The use of the model will be demonstrated for prostate, cervix, and lung cancer planning.

## METHODS AND MATERIALS

### *Parameters required*

Since the geometrical uncertainties of an individual patient who is to be planned are not known, measured data of a group of similar patients must be used. Clinical studies performed in our department and elsewhere have shown that translational deviations in patient positioning of a specific group can be approximated by normal distributions of systematic and random deviations in the three main directions (e.g., 2, 3). For each patient in the study the average setup deviation and the standard deviation (SD) of the distribution around that average is determined. The random variation  $\sigma$  characterizing a certain patient group is then defined as the SD of the day-to-day setup positions, averaged over all patients in the group. The systematic variation  $\Sigma$  is defined as the SD of the distribution of average setup deviations per patient in the group of patients. The overall mean deviation  $M$  is the average value over all fractions and all patients. If the reference setup (during simulation) can be considered as a sample from the random distribution,  $M$  will be close to zero and  $\Sigma$  will be close to  $\sigma$ . Rotational deviations around the three main axes can in principle be described similarly.

The study of internal organ motion can yield random and systematic deviations for translations and rotations as well. Hence a set of 12 (x/y/z \* rot/trans \* int/ext) standard deviations  $\Sigma$  and  $\sigma$  and six rotation axes are necessary to describe all geometrical uncertainties of a specific patient group. These values are the input parameters of our method and do not only depend on the tumor sites, but also on setup techniques and treatment protocols (and possibly even on more specific variables like tumor stage, patient weight, accelerator, etc.).

The parameters are used to calculate margins around a CTV which is initially represented by a set of input contours as outlined in 2D CT slices. The contour data points are used to determine a 3D volume in a cubic calculation grid in the treatment room (i.e., CT) coordinate system. The algorithm has been described before (25) and can be summarized as follows. For each slice, intersection points of contour lines with 2D grid lines are calculated to fill a 2D matrix with values equal to the fraction of the grid element that is enclosed by the contour. The slices are stacked with increasing slice position so that a 3D matrix  $M_{CTV}(x,y,z)$  is created with values 1 inside the volume and 0 outside the volume (and between 0 and 1 at the edge). This matrix is used for subsequent calculations.

#### Coverage probability calculation using convolutions

Two separate, equivalent methods have been developed to calculate a matrix with coverage probabilities (CPs) which is defined as the probability for each point to be covered by the CTV and which will be used for PTV margin determination. They will be designated as the convolution method and the Monte Carlo method. The *convolution method* uses a straightforward convolution of the CTV matrix with normal distributions describing the geometrical uncertainties. The effect of translational and rotational deviations is calculated separately. The normal distribution of mutually independent deviations in translations is given by:

$$N(x,y,z) = \frac{e^{-\frac{1}{2} \cdot \left( \left( \frac{x}{sd_x} \right)^2 + \left( \frac{y}{sd_y} \right)^2 + \left( \frac{z}{sd_z} \right)^2 \right)}}{\sqrt{8\pi^3} \cdot sd_x \cdot sd_y \cdot sd_z} \quad (1)$$

with  $sd_x$ ,  $sd_y$ , and  $sd_z$  the standard deviations of the distributions in the three main directions. The input matrix  $M_{CTV}(x,y,z)$  is convolved numerically with the probability distribution:

$$M_{CP}(x,y,z) = \sum_{x'} \sum_{y'} \sum_{z'} M_{CTV}(x',y',z') N(x-x', y-y', z-z') \Delta x \Delta y \Delta z \quad (2)$$

with  $\Delta x \Delta y \Delta z$  the voxel size. In the output matrix  $M_{CP}(x,y,z)$  the original contents of the voxels is spread out according to the distribution of translations. The value in each voxel of this “coverage probability” matrix represents the probability of the voxel being covered by the CTV.

Inclusion of rotational positioning deviations is cumbersome in the orthogonal coordinate system. To be able to handle rotations around axes in the three main directions, an input matrix  $M_{CTV}(x,y,z)$  is transformed to cylindrical coordinates  $M_{CTV}(r,\vartheta,a)$  using bilinear interpolations, where  $a$  is  $x$ ,  $y$ , or  $z$  for rotations about  $x$ -,  $y$ -, or  $z$ -axis respectively. The center of the new matrix ( $r = 0$ ) is taken to be at the (user-defined) position of the rotation axis. A one-dimensional distribution matrix  $N(\vartheta)$  is defined similar to  $N(x,y,z)$  and the convolution is performed:

$$M_{CP}(r,\vartheta,a) = \sum_{\vartheta'} M_{CTV}(r,\vartheta',a) N(\vartheta - \vartheta') \Delta \vartheta \quad (3)$$

with  $\Delta \vartheta$  the bin size. Subsequently the output matrix  $M_{CP}(r,\vartheta,a)$  is transformed back to orthogonal coordinates  $M_{CP}(x,y,z)$ . The transformation to a different coordinate system and back, on a discrete grid, will already smooth the CTV matrix, even without convolutions. To limit this effect, the pixel size in the cylindrical coordinate system is kept four times smaller than in the original. To minimize the number of cylindrical matrix elements and keep the element size approximately equal for all values of  $r$ , the number of angles  $\vartheta$  increases with  $r$ , i.e., the  $(r,\vartheta)$ -calculation grid is not rectangular but rather triangular in shape.

In case more than one rotational deviation is present, the above procedure is performed again using the output matrix of the first calculation as input for the second, etc. The order is arbitrary for distributions that are mutually independent and for the small rotational deviations ( $< 10^\circ$ ) that are usual in patient setup and organ movement (as will be justified later on, see Fig. 4). In case both rotational and translational deviations must be considered, the rotations should be performed first.

#### Coverage probability calculation using a Monte Carlo approach

The *Monte Carlo method* simulates the fractionated radiotherapy treatment more directly by sampling the translations  $t_x$ ,  $t_y$ ,  $t_z$  and rotations  $r_x$ ,  $r_y$ ,  $r_z$  from their respective distributions. Subsequently all points in the CTV matrix  $(x,y,z)$  are moved to a new position  $(x',y',z')$  according to:

$$\begin{aligned} x' &= x + t_x + x_{r,y}(\cos(r_y) - 1) + x_{r,z}(\cos(r_z) - 1) \\ &\quad - y_{r,z}\sin(r_z) + z_{r,y}\sin(r_y) \\ y' &= y + t_y + y_{r,z}(\cos(r_z) - 1) + y_{r,x}(\cos(r_x) - 1) \\ &\quad - z_{r,x}\sin(r_x) + x_{r,z}\sin(r_z) \\ z' &= z + t_z + z_{r,x}(\cos(r_x) - 1) + z_{r,y}(\cos(r_y) - 1) \\ &\quad - x_{r,y}\sin(r_y) + y_{r,x}\sin(r_x) \end{aligned} \quad (4)$$

where  $x_{r,y} = (x - R_{x,y})$ ,  $x_{r,z} = (x - R_{x,z})$ , etc. the coordinates of the matrix point with respect to the  $x$ -,  $y$ -, and  $z$ -axes of rotation, respectively  $(R_{y,x}, R_{z,x})$ ,  $(R_{x,y}, R_{z,y})$ ,  $(R_{x,z}, R_{y,z})$ . The input value at point  $(x,y,z)$  can be assigned to the eight grid

points nearest to  $(x', y', z')$  using trilinear interpolations or assigned completely to the one nearest point which is faster but less accurate. Hence a new matrix  $M_n(x, y, z)$  is calculated with  $n$  being the sample number. The procedure is repeated many times ( $> 1000$ ) and the resulting matrices  $M_n(x, y, z)$  are averaged over the number of samples to yield the final result  $M_{CP}(x, y, z)$ .

A difference between Monte Carlo and convolution method is the way in which rotational deviations are incorporated. The Monte Carlo method handles all rotations at once. The voxel displacement resulting from each rotation is calculated assuming the same starting position for all rotations, i.e., the input voxel position for the second rotation is not the output from the first. The computation of translations is similar for both methods; all three directions are handled simultaneously. Comparison of the methods will give an indication of their accuracy.

#### Interpretation of coverage probability

As mentioned before, the elements in the CP matrix  $M_{CP}$  (of which the values vary from 0 to 1) represent the probability of a fixed point in space to be actually covered by the CTV. For sufficiently large volumes (larger in diameter than about 2 SD of the distribution of deviations), the CP value of a certain voxel also represents the probability that the volume border lies outside that voxel; i.e., if a point is covered by some part of the CTV, the CTV border must lie outside of that point (or exactly on it). Iso-coverage probability volumes are therefore logical candidates to define the PTV. Considering translational deviations in one dimension and given a selected coverage probability  $CP_s$  smaller than 0.5, the probability ( $P_o$ ) that any point of the CTV volume is outside the PTV will then be equal to  $2 CP_s$ . For translations in more dimensions and for rotations, the relationship between  $CP_s$  or the margin size and  $P_o$  becomes less straightforward. A special case may however serve as an estimate for the general case.

That special case is a spherical CTV with an isotropic margin  $m$  to represent the PTV. The probability  $P_o$  that any point of a CTV with normally distributed translational deviations  $sd$  in all three dimensions will be outside the PTV can be calculated analytically:

$$P_o = \frac{2}{\sqrt{2\pi}} \int_{r>m/sd} r^2 e^{-\frac{1}{2}r^2} dr \quad (5)$$

with  $r$  being equal to  $\sqrt{(x^2 + y^2 + z^2)}$ . The integral can be solved using partial integration. For deviations in two dimensions a similar expression can be derived. In Fig. 1  $P_o$  is displayed as a function of the margin in units of  $sd$ , for the one-, two-, and three-dimensional case. The coverage probability values  $CP_s$  that should be selected to obtain a margin  $m(sd)$  are displayed along the upper horizontal axis. The relation between  $CP_s$  and  $m(sd)$  is normally independent of CTV shape as long as the volume is sufficiently large ( $> 2 sd$ , as indicated before). For 3D translational deviations, the

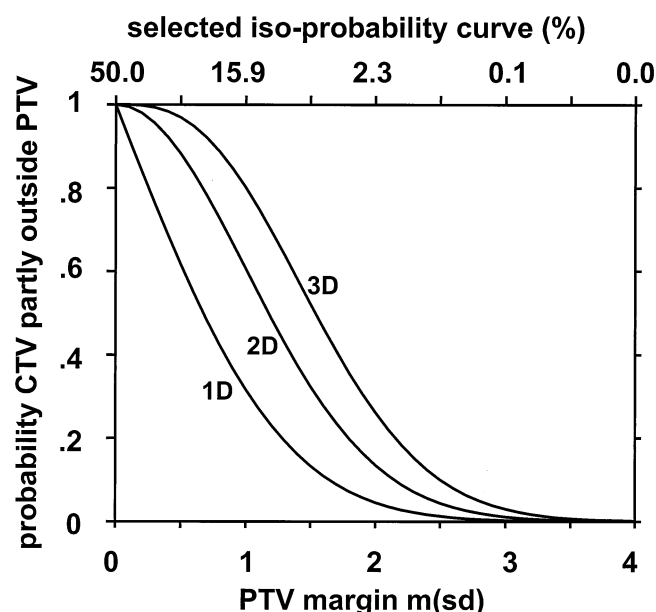


Fig. 1. Theoretical curves for a spherical CTV with variations in translations with standard deviations  $sd$ . Rotational variations are zero. Indicated is the probability that the CTV is partly outside the PTV ( $P_o$ ) for variations in one, two, and three dimensions with varying CTV-to-PTV margin size in units of  $sd$ . The corresponding selected iso-probability values ( $CP_s$ ) are indicated on the upper horizontal axis.

probability of the CTV being partly outside the PTV is considerably higher than for 1D deviations. For instance, a PTV margin of 1  $sd$  (or  $CP_s = 16\%$ ) has a  $P_o$ -value of 32% for deviations in one dimension as opposed to 80% when deviations in all three dimensions are considered. However, not only the probability of CTV miss but also the extent of that miss is important. Even for large  $P_o$ -values, the fraction of the CTV outside the PTV is small and the dosimetrical consequences are limited.

#### Influence of systematic deviations on the CTV dose: dose probability histograms

To investigate the effect of the geometrical uncertainties on the dose distribution in the CTV, different approaches for systematic and random deviations are required. Systematic geometrical misses will cause underdosage of the same part of the CTV for every fraction of the treatment, whereas random deviations will cause underdosage in different parts of the CTV for each fraction. For systematic deviations, the CP matrix can be used to estimate the influence of systematic deviations on the DVH of the CTV. A normal cumulative DVH is constructed by summation of all CTV voxels that receive more than a certain dose, for all dose values  $D$ :

$$V(D) = \sum_{\vec{r} \in CTV} S_D(D'(\vec{r})) \Delta V = \Delta V \sum_{\vec{r} \in \mathbb{R}^3} S_D(D'(\vec{r})) M_{CTV}(\vec{r}) \quad (6)$$

$$\text{with } S_D(D'(\vec{r})) = \begin{cases} 1 & \text{for } D'(\vec{r}) \geq D \\ 0 & \text{for } D'(\vec{r}) < D \end{cases}$$



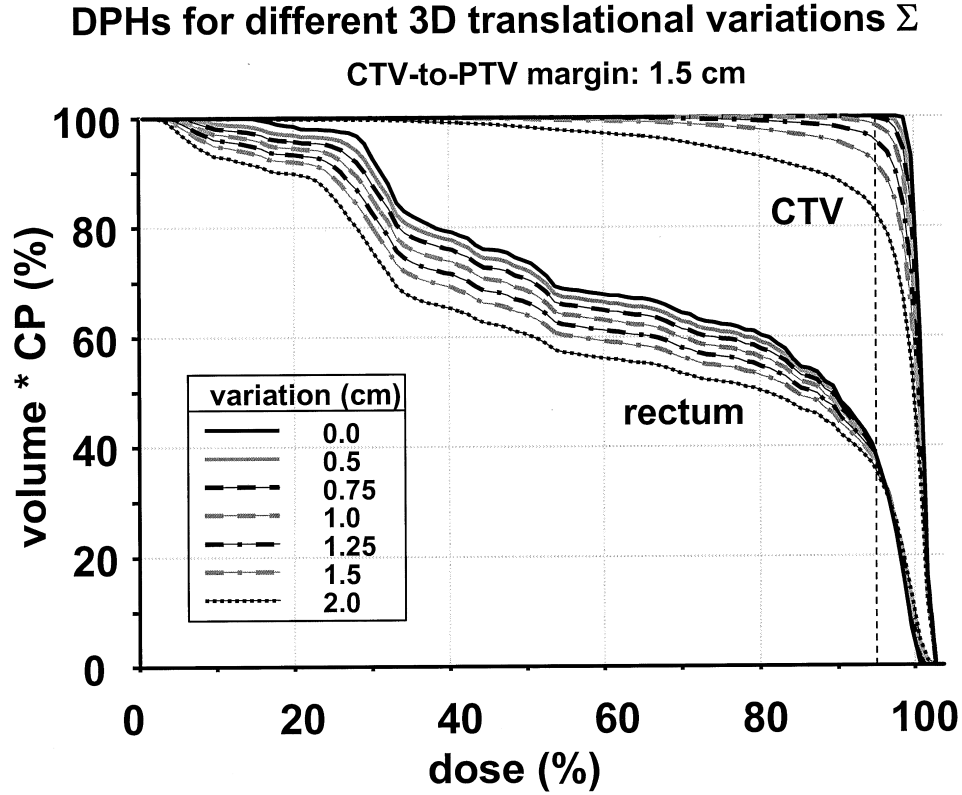


Fig. 2. Example of dose probability histograms for six different systematic variations in translation ( $\Sigma$ ) for a prostate case planned to conform to ICRU recommendations with a 1.5 cm CTV-to-PTV margin. With increasing variation in CTV position there will be a higher probability of underdosage. The rectum will on average also receive less dose as the variations increase, although the maximum dose increases.

with  $D'(\tilde{r})$  the dose value at position  $\tilde{r}$ ,  $\Delta V$  the voxel volume, and  $M_{CTV}(\tilde{r})$  the previously defined CTV matrix.  $\tilde{r} \in CTV$  and  $\tilde{r} \in \mathbb{R}_3$  are those positions which are member of the CTV and the whole 3D space, respectively. At the time of planning the systematical deviations in CTV position are unknown for a specific patient but the probability of the CTV being systematically at a different position is determined by the systematic variations  $\Sigma$  of translations and rotations for the patient group. The average DVH, taking all systematic deviations of the CTV position with respect to the dose distribution into account, can then be determined to be:

$$\begin{aligned}
 \langle V(D) \rangle &= \Delta V \sum_{\tilde{r} \in \mathbb{R}_6} N(\tilde{t}) \sum_{\tilde{r} \in \mathbb{R}_3} S_D(D'(\tilde{r})) M_{\tilde{r}(CTV)}(\tilde{r}) \\
 &= \Delta V \sum_{\tilde{r} \in \mathbb{R}_3} S_D(D'(\tilde{r})) \sum_{\tilde{t} \in \mathbb{R}_6} N(\tilde{t}) M_{\tilde{r}(CTV)}(\tilde{r}) \quad (7) \\
 &= \Delta V \sum_{\tilde{r} \in \mathbb{R}_3} S_D(D'(\tilde{r})) M_{CP}(\tilde{r})
 \end{aligned}$$

with  $\tilde{t}$  being a transformation (translations and rotations),  $N(\tilde{t})$  the probability for a certain transformation  $\tilde{t}$  (see Eq. 1), and  $M_{\tilde{r}(CTV)}$  the transformed CTV. In the last step of the derivation Eq. 2 is used. Hence instead of counting voxels receiving a dose  $\geq D$ , as for a normal DVH, the average of

the DVH for all systematic deviations of the CTV is obtained by summation of the coverage probability values for each dose  $\geq D$ . Therefore the results of those calculations will be denoted as dose probability histograms (DPHs). It should be emphasized that the CP matrix  $M_{CP}$  in Eq. 7 is calculated using the *systematic* variations  $\Sigma$ . A dose histogram of a CP matrix for random (day-to-day) variations of one patient has no physical meaning since DVHs of different fractions should not be added; information about the position of the dose, which is essential when adding dose distributions of different days, is lost in a DVH.

In Fig. 2 a clinical example of DPH calculations is shown. For an arbitrary prostate cancer patient planned according to the ICRU dose specification rules (i.e., block margins are such that the 95% isodose volume encloses the PTV), DPHs of CTV have been calculated for six different 3D translational variations  $\Sigma$ . Naturally, the probability of CTV underdosage increases with increasing variations. Since the ICRU suggested a maximal tumor underdosage of 5% (1), an additional dashed line is drawn to indicate the 95% dose. The DPH curves for the CTV now immediately indicate that the 95% isodose will enclose on average a large part of the CTV ( $>$  about 99%) as long as the CTV-PTV margin is at least  $2\Sigma$ . This implies a high probability of the 95% isodose enclosing the whole of the PTV. For smaller margins there will be an increasing probability

of underdosage of the CTV. The DPH as an average of the DVHs for all systematic deviations seems therefore a reliable tool to determine the margin size required to cover for these deviations for a specific treatment plan. Also indicated in Fig. 2 are similar curves for variation in rectum position. The same variations are assumed without any change in rectum shape. As expected, the maximum dose of the DPH increases as the variations increase; the probability that the rectum will be part of the higher dose regions will be higher. At the same time, however, the lower dose volumes decrease with increasing variations. This is due to the fact that for isotropic movements in all directions, the probability of the rectum moving toward the higher dose regions is lower than for moving away from these regions.

#### *Influence of random deviations on the CTV dose*

The *random* deviations displace the CTV with respect to the dose distribution differently for each fraction of the treatment. This can be simulated by convolution of the dose distribution matrix with the probability distributions, as has been described before (17, 18, 26, 27). The same algorithms as for the CP calculations can be applied. If the input file in Eq. 2 ( $M_{CTV}$ ) is a dose distribution instead of the CTV, the output will be a dose distribution which is spread out locally as a result of random deviations. This distribution is the best estimate of the actually delivered distribution during the radiotherapy treatment. In general the higher isodose regions will decrease in size, while the lower isodose regions will increase. The extent of shrinkage of the 95% isodose volumes should give an indication for the size of the required margin (26). If only the random *setup* deviations are considered, one calculation will be sufficient to determine its effect on CTV and critical organs simultaneously. If the internal random deviations of the critical organs are different for different organs, separate convolutions of the combined distributions of random setup and organ movement should be performed with the local dose matrix surrounding each organ. Compared to CP calculations, dose modifications are more accurate because gradients in dose matrices are considerably flatter than those in CTV matrices.

#### *PTV margin determination*

The goal of a PTV is to create a volume around which the 95% dose can be planned so that the CTV is adequately irradiated, which can be verified using DPHs (see next section). In principle one might find the correct PTV by trial and error but CP calculations can also be used to calculate a good PTV to start with. Because of the different effect of the systematic and random deviations on the CTV dose ( $\Sigma$  and  $\sigma$  cannot be added), the PTV is calculated in two steps.

For *systematic* geometrical uncertainties a high irradiation probability is obtained by choosing the margin according to a low iso-probability volume. From Fig. 2 a margin equal to about  $2\Sigma$  would seem reasonable and from the upper horizontal axis in Fig. 1 it can be deduced that this corresponds to iso-probability curves of about 2.5%. Hence the first step in the PTV calculation (PTV1) is the determi-

nation of the 2.5% iso-probability volume of the CTV (i.e., the volume bounded by voxels having a CP equal to 2.5%), using the systematic variations  $\Sigma$  as input to the model. From Fig. 1 this implies that for a spherically symmetric situation and deviations in all directions, there still is at least a 28% chance that a part of the CTV is outside PTV1 for all fractions. In other words, there is maximally a 72% probability of complete enclosure of the CTV by the PTV1 during the radiotherapy treatment. However, the DPH curves of the example in Fig. 2 indicate that the 95% isodose will enclose the CTV in practically all cases. The internal and external deviations can be handled simultaneously by adding the respective standard deviations in quadrature.

To cover for the remaining *random* deviations, only a moderate increase in the margin will be necessary. The total random variation equals the quadratic sum of in- and external random variations. The procedure is similar to that for the systematic deviations, this time using PTV1 instead of the CTV as input volume. The difference is that random deviations do not affect the dose distribution in the tumor as much as systematic deviations. Therefore the margins can be smaller and the selected iso-probability volume can be higher. Bel *et al.* studied the dosimetric consequences of random translational variations  $\sigma$  for their prostate patients and concluded that a  $0.7\sigma$  margin would be sufficient to keep the minimal CTV dose above 95% (26). Based on those results we considered the 25% iso-probability volume appropriate for random deviations. This means that PTV1 will be partly outside the PTV in over 90% of the fractions (see Fig. 1). Once this final margin is added to PTV1, the calculation of the PTV is complete. Naturally, the choice of the iso-probability volume for either PTV1 or PTV margins is to some extent arbitrary and can be varied according to the individual preferences of the clinician. Eventually it should be based on quantitative models for the tumor control probability.

#### *PTV margin verification*

Normally, the patient will be planned with certain block margins around the PTV to account for the penumbra of the beam. The concepts described can be applied to evaluate and judge the effect of geometrical uncertainties on the dose distribution in the CTV. Firstly, to calculate the expected dose distribution actually delivered during the treatment series, the dose matrix is convolved with the distribution of random deviations. The 95% isodose volume will shrink but should still enclose the PTV1 volume. Secondly the systematic deviations are used to determine the DPH of the CTV (and possibly critical organs), using the dose modified for random deviations. This DPH indicates whether the dose distribution is adequate to irradiate the CTV, given the systematic and random deviations. If the patient has been planned correctly, the average CTV volume receiving > 95% dose must be high (e.g., > 99%). In case the probability of underdosage is too high, the 95% isodose volume is too tight around the CTV and either the PTV margin or the block margin is too small. The plan can be recalculated

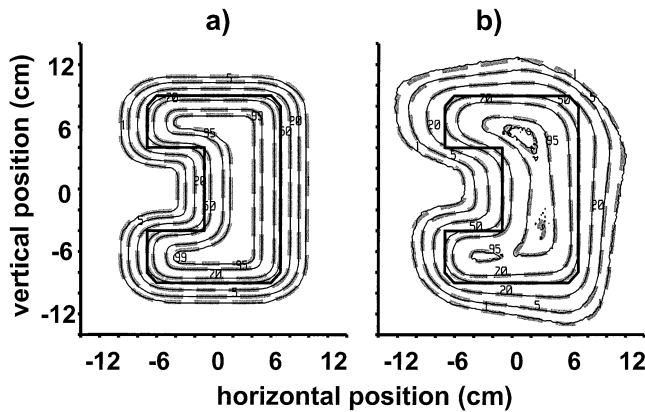


Fig. 3. Comparison of convolution and Monte Carlo method. The schematic 2D CTV is the object outlined by the thick solid contour, the pixel size is 2 by 2 mm. (a) A horizontal 12-mm (1 SD) and vertical 8-mm variation in translation has been simulated. The 1, 5, 20, 50, 70, 95, and 99% iso-probability curves of both methods are shown; the thin black lines represent the result of the Monte Carlo method (1500 runs), the thick gray dashes the convolution method. (b) A 5° (1 SD) variation in rotation is added. The rotation axis is at the lower left corner of the figure (−12, −12 cm). The iso-probability curves of the two methods still coincide well.

using lower iso-probability contours as PTV margin or larger block margins. In case the DPH is practically equal to the original DVH (i.e., systematic deviations have no influence on the dose in the CTV), the PTV margins might be too large and the plan should be recalculated using higher iso-probability values as PTV margins (or smaller block margins). In this iterative manner the size of the block-to-CTV margins is directly optimized for irradiation of a specific CTV, and DPHs of CTV instead of DVHs of PTV are used to evaluate the planning.

#### Hardware

The method has been implemented using the C programming language on a HP 9000/712 (100 MHz) workstation. It runs as a separate application next to the CADPLAN planning system (Varian-Dosetek) and hence uses CADPLAN contour and dose files as input. The results are written back to CADPLAN files for visualization and further planning. At the moment, the voxel sizes in the calculations are equal to those used in the planning system, which vary in practice from about 2 mm for CT pixel size to maximally 10 mm for the slice distances. The dose matrices normally have a resolution of 2.5 or 5 mm. Geometrical uncertainties smaller than about 1 mm (1 SD) are consequently not reflected in the calculations.

## RESULTS

#### Accuracy of the methods

To get an indication of the accuracy of the convolution and Monte Carlo method, results of the two methods are compared for a schematic example. Figure 3a depicts a 2D

geometrical object which represents a target volume. The simulated random translational variations are different in horizontal and vertical direction and the coverage probabilities are calculated for both methods. The number of runs in the Monte Carlo method was 1500. The iso-probability contours of the different methods coincide well, only the 1% iso-probability curves deviate slightly. In Fig. 3b an additional variation in rotation is simulated. As expected, the area within the higher probability curves decreases whereas that in the lower increases. Due to the rotations the distance from one curve to the next becomes anisotropic. Near the upper right part of the object the lower iso-probability curves actually shrink compared to the curves in Fig. 3a; because of the rotations there is a lower probability that voxels in that area are enclosed by the object. The differences between the two methods become slightly larger, especially near the low probability curves. This is attributed to the limited number of runs of the Monte Carlo method which yields poor statistics in those regions.

The largest differences between the two CP calculation methods are expected for coverage probability calculations with large rotational deviations. Hence an exaggerated (and unrealistic) variation in rotations around the three orthogonal axes through a point in the lower left and cranial corner of the input matrix is calculated for a lung tumor CTV in the upper thorax. Figure 4 shows the 5% iso-probability curves for both methods in a transversal, sagittal, and frontal slice near the center of the CTV. The two contours do not overlap in all areas but the differences are small: maximally 2 mm (1 CT pixel) while the margin is on average 2 cm. In slices near the edges of the volume the maximum differences that are found are 4 mm which is adequate considering the irregularity of the Monte Carlo contours. The difference between the two 5% iso-probability volumes is 4 cc (1%). In clinical practice rotational deviations of extreme values are rare and the occurrence of more than one deviation simultaneously is unlikely. Consequently, this close agreement may serve as assurance that the calculation of rotational deviations is reliable for both methods.

Although Eq. 5 was derived for a spherically symmetric case, the results are a reasonable approximation for more general clinical situations. For translational deviations, computer simulations for a prostate CTV indicate that, even if the margins become anisotropic, the deviations from the values in Fig. 1 are small (< 5%). A restriction is that the CTV volume should be devoid of sharp edges, which is usually satisfied. Another limitation is that rotational deviations are not included in the calculations, hence Eq. 5 underestimates the  $P_o$ -value if rotations are present.

#### Clinical examples

In three clinical examples the stepwise PTV calculation and the verification procedure will be illustrated. The values for the geometrical uncertainties are taken from literature or have been measured in our institute. In all cases it is assumed that the application of an off-line protocol (as

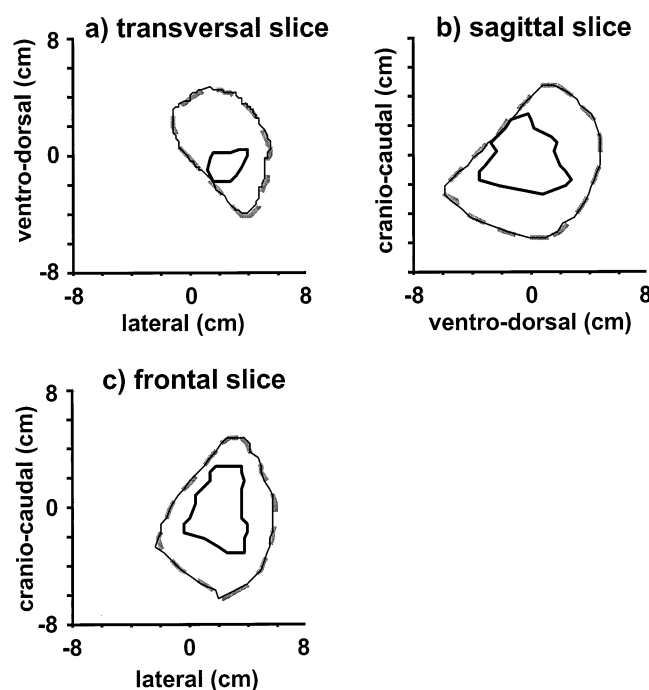


Fig. 4. Comparison of the two methods for an extreme case of rotational deviations. A lung CTV (thick black lines) has been modified with rotational deviations of 10°, 8°, and 6° (1 SD) around the three major axes in a point about 8 cm left, cranial, and below the CTV center. The 5% iso-probability curves for the convolution (thick gray dashes) and Monte Carlo method (thin black lines) are displayed in a transversal (a), sagittal (b), and frontal cut (c) through the CTV. Although the two methods handle the effect of rotational deviations differently, the results are quite similar.

mentioned in the introduction) halves the systematic translational setup deviations (4). The values used are summarized in Table 1. All calculations are done with the convolution method and all rotation axes are through the center of the CTV unless specifically stated otherwise. CT slice distances are 5 mm and CT pixel size are about  $2 \times 2$  mm. The grid size of the dose matrices is in all cases 2.5 mm in the plane of the CT slices and equal to the CT slice distance in the direction perpendicular to the CT planes. All three patients were planned with multileaf collimators. Block margins were such that the 95% isodose closely fitted the PTV and the dose homogeneity in the PTV satisfied the ICRU 50 recommendations (i.e., dose variation of maximally 95%–107%).

#### Prostate cancer case

Due to variations in rectum and bladder filling, the range of the internal prostate movements is considerable. The values that are used in our calculations have been estimated from several studies available in the literature (9, 10, 12). The lateral rotation axis was taken to be near the apex of the prostate as suggested by van Herk *et al.* (12). The values for external setup deviations are taken from routine portal imaging data of 228 patients treated at our clinic. The final

Table 1. Overview of geometrical uncertainties used as input for the model for three different tumor sites\*

Variation	Translations (mm, 1 SD)			Rotations (degrees, 1 SD)/axis		
	lateral	cran-caud	vent-dors	lateral	cran-caud	vent-dors
<b>Prostate</b>						
$\sigma$ ext	2.0	2.0	2.0	1	1	1
$\Sigma$ ext	1.2	1.2	1.4	1	1	1
$\sigma$ int	1	2	2	4 <sup>†</sup>	2	1
$\Sigma$ int	1	2	2	4 <sup>†</sup>	2	1
<b>Cervix</b>						
$\sigma$ ext	3.5	4.0	3.5	3	1.5	2
$\Sigma$ ext	2.0	2.5	2.0	2	1	1
$\sigma$ int	1	1	1	1	1	1
$\Sigma$ int	1	1	1	1	1	1
<b>Lung</b>						
$\sigma$ ext	3.0	3.0	3.0	2	2	2
$\Sigma$ ext	2.0	2.0	2.0	1	1	1
$\sigma$ int	4	5	5	2	2	2
$\Sigma$ int	2	3	3	1	1	1

\* Systematical ( $\Sigma$ ) and random ( $\sigma$ ) variations are indicated for translations as well as rotations and internal organ movement (int) as well as external setup deviations (ext). All rotation axes are assumed to be at the center of the CTV except for those indicated by <sup>†</sup> which are assumed to be at the caudal apex of the CTV.

PTV is constructed in several steps as shown in transversal and sagittal slices through the tumor (Fig. 5). The CTV has been outlined manually by a radiation oncologist. This volume is expanded with a margin to cover all systematic deviations; a CP matrix is calculated using the quadratically summed internal and external systematic variations (Table 1). PTV1 is taken to be the volume enclosed by the 2.5% iso-probability contours. To get the final PTV a subsequent margin is added to PTV1 from the calculated 25% iso-probability volume with the quadratically summed random variations as input for the CP calculations. The random deviations add only an extra 1–2 mm (which is close to the pixel size). In total, the margin around the CTV varies from minimally 6 in the caudal to maximally 13 mm in the cranial region of the PTV. The anisotropy is due to the significant rotation around the apex of the prostate.

The interpretation of the contours in the two-dimensional slices is sometimes misleading due to the 3D aspect of the margins; they may appear too large in one slice due to the influence of a differently shaped tumor contour in the next slice, as is especially apparent in the (cranial) transversal slice. This effect is also visible in the cervix and lung cancer cases that follow.

A three-field technique was applied to plan the patient. To verify the dose distribution in CTV, rectum, and bladder, DVHs have been calculated for each volume and are shown in Fig. 6. Subsequently, the dose distributions around the volumes of interest have been convolved with the distributions of random deviations. For the CTV the values are directly obtained from Table 1, for bladder and rectum the internal random motion was estimated to be equal to that of



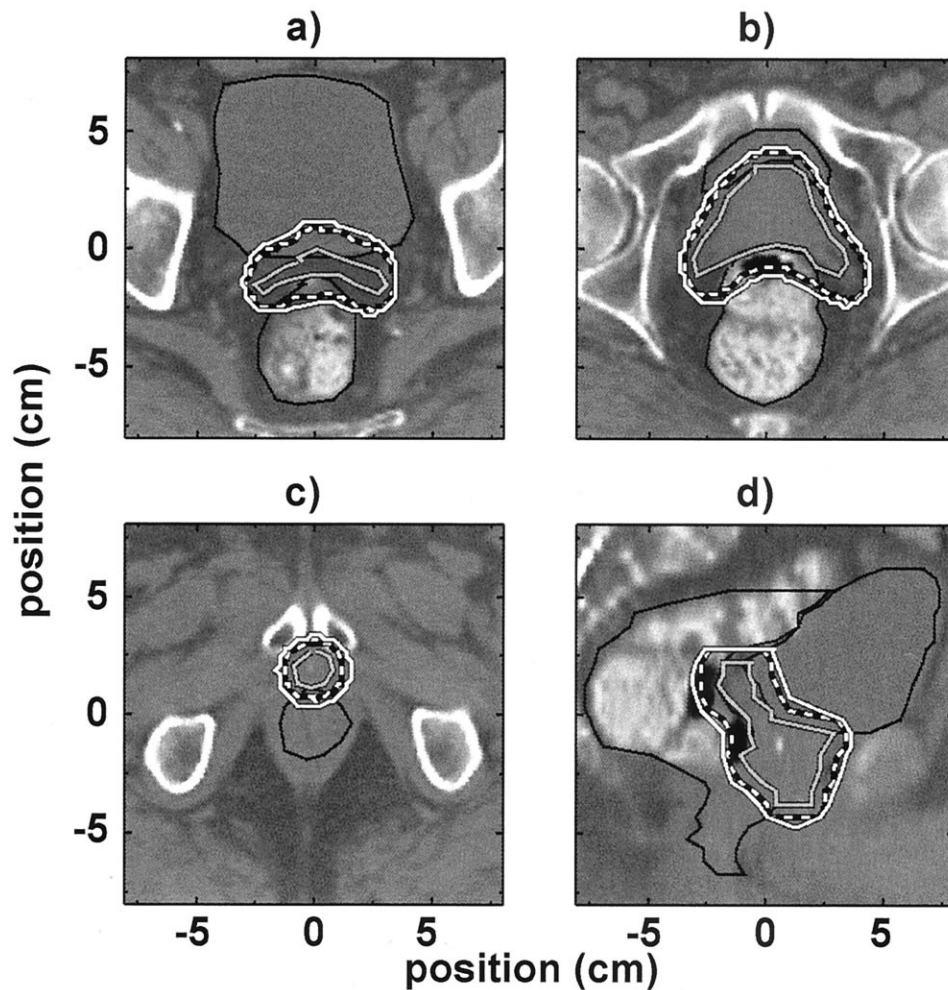


Fig. 5. Prostate planning example of the stepwise PTV calculation in a cranial transversal slice (a), an isocentric slice (b), a caudal slice (c), and a sagittal reconstruction (d). The geometrical uncertainties are from Table 1. The CTV (gray curve) is extended with a margin to cover for the systematic deviations by selection of the 2.5% iso-probability volume of the CP matrix (PTV1, dashed curve). The final PTV (white curve) results from the 25% iso-probability volume of the CP matrix of random deviations applied to the PTV1. Especially in the sagittal slice the influence of the rotations around the apex is clear; the PTV margin in the caudal part is significantly smaller than that in the cranial part of the prostate. The critical organs (bladder and rectum) are depicted by the thin black curves.

the prostate without the rotation. Bladder and rectum volumes were assumed to be constant. Resulting DVHs show that the effect of random deviations on the CTV dose is negligible, whereas the bladder and rectum high dose volumes are somewhat reduced. Finally, the DPHs for the systematic deviations have been determined using the dose distributions modified for random uncertainties. Standard deviations are taken from Table 1 similar to the random deviations. The DPH of the CTV is different from the original DVH but the DPH-curve does not quite intersect the 95% dose line, i.e., the probability of underdosage of the CTV is negligible. The DPHs for the critical organs do not deviate from the DVHs.

#### Cervix cancer case

Compared to prostate cancer patients, external setup deviations play a major role in the planning of (postoperative)

gynecological cancer patients. Positioning accuracies of cervix cancer patients are also determined by studies in our own institute, one of which is described by Creutzberg *et al.* (3). Also in contrast with the prostate case, the internal organ movement is expected to be relatively small considering the involved anatomy. In Fig. 7 four slices through the initially drawn CTV are depicted. The PTV1 margins due to systematic deviations are calculated similar to the prostate case and vary from 6 to 9 mm. They are mainly caused by the external deviations. The addition of a margin for random deviations completes the PTV calculation. The final CTV-to-PTV margin is then about 1 cm. An additional feature of margin calculation using coverage probabilities is the smoothness of the PTV surface. This especially manifests itself in the sagittal view in Fig. 7d; the inconsistencies in the CTV delineation disappear in the PTV.

The patient was planned in prone position with a three-

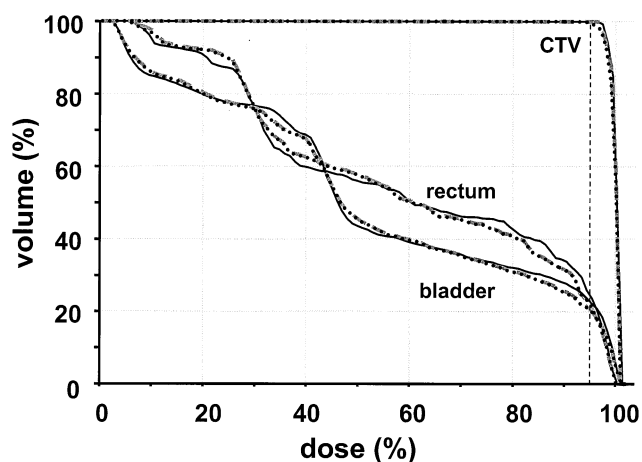


Fig. 6. DVHs and DPHs for the prostate cancer patient in Fig. 5. The original DVHs of CTV, bladder, and rectum are indicated by the thin black lines. DVHs for the dose distributions adjusted for random deviations are represented by the dashed gray curves. The effect of random deviations on the CTV dose is negligible, whereas the bladder and rectum high dose volumes decrease. The DPHs (dotted curves) for the systematic deviations have been determined using the dose distributions modified for random uncertainties. There is only a noticeable effect on the CTV but the curve does not intersect the 95% dose line (dashed) so the probability of underdosage of the CTV is negligible.

field technique. The relatively large random positioning deviations are solely responsible for the random deviations. DVHs and DPHs for CTV, small bowel, and rectum have been calculated similar to the prostate case. The results are shown in Fig. 8. The effect of the random uncertainties on the rectum and small bowel is again a noticeable reduction of the high dose volume. The original DVH of the CTV indicates a less homogeneous dose distribution than for the prostate case. It is, however, hardly influenced by the systematic or random deviations and the final DPH proves that adequate margins have been applied.

#### Lung cancer case

A last example is a 3-field lung booster plan designed to spare the right lung (Fig. 9). Due to breathing and cardiac motion there is considerable internal tumor movement the magnitude of which has been estimated from previously published values (13). Values for external setup deviations are based on the preliminary results of a lung cancer patient positioning study recently conducted in our own institute. The manually outlined CTV is expanded with a 6–9 mm margin to cover internal and external systematic deviations. The random deviations require an additional 3–5 mm margin for the final PTV and the total margin becomes 10–13 mm.

Variations in position of the lungs and the spinal cord are assumed to consist only of setup deviations. In the DVHs of CTV and left lung the random-deviation-adjusted dose distributions display similar differences with the original as the cervix cancer case (Fig. 10). However, the spinal cord is an exception. Since the beams in the three-field plan are positioned (too) close to the spinal cord, there is a strong dose

gradient just next to it causing an increase of spinal cord dose in the random-deviation-adjusted plan. To a lesser degree the same holds for the right lung. The DPHs for the critical organs are again practically equal to the DVHs, except for the spinal cord; due to the position of the beams the systematic movements of the spinal cord cause a (slight) increase in average spinal cord volume receiving high dose. The DPH of the CTV is different from the DVHs but the high probability of sufficient dose homogeneity indicates that the PTV and block margins were adequate.

#### Computer performance

The calculation speed depends on the selected method and input. The margin and DPH calculations normally take about 1–2 minutes with the convolution method. Generally the Monte Carlo method is about three to six times slower since a large number ( $> 1000$ ) of samples have to be taken to obtain sufficient accuracy in the low probability regions. Therefore the Monte Carlo method is only used for verification in case of questionable results. For both methods the computation time increases linearly with the size of the input and convolution matrices. Since the dose matrices are currently fixed to the standard CADPLAN format ( $160 \times 112 \times$  number of slices), dose modifications are slower. (In principle only that part of the dose matrix that surrounds the volume of interest needs to be included in the calculations). Besides, almost all elements of the dose matrix are nonzero whereas volume matrices contain a substantial part of zero elements that are ignored in the calculations. The normal time required for dose modifications with the convolution method varies from 2 (without rotations) to about 10 minutes which is a fraction of the time needed for volumetric dose calculations. Hence the method is sufficiently fast to be used in the iterative planning process.

## DISCUSSION

#### Margin calculations

The methods proposed in this paper will be particularly useful for designing PTV margins in case of new conformal therapy studies. Based on knowledge (or intelligent guesses) of a set of standard deviations describing all possible geometrical uncertainties of the CTV position, the CP values will give an indication where the CTV of an individual patient will be positioned over the course of treatment. However, repeated calculations within a specific patient group will normally yield equal margins for all patients independent of the shape of the CTV. For normally distributed deviations and in absence of significant rotational deviations, our choice of iso-probability volumes, which is based on the assumption that on average a high percentage of the CTV volume ( $> 99\%$ ) should receive a high dose ( $> 95\%$ ), yields margins of about  $2\sigma + 0.7\sigma$ . Consequently, the margins might also be applied directly to the CTV by straightforward CTV expansion algorithms (23–25), without having to perform the CP calculations each time.

One difference between rigid margin addition and the CP method might reveal itself at sharp edges. If no smoothing

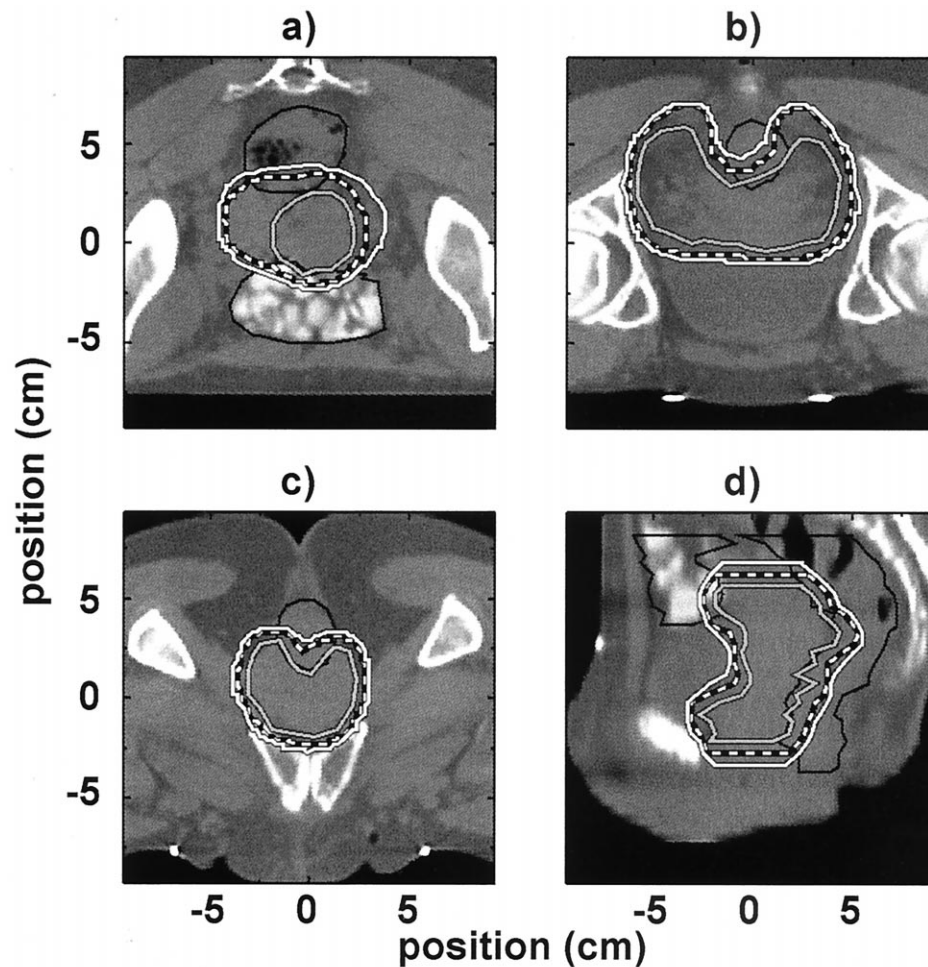


Fig. 7. Example of the PTV calculation for a cervix cancer plan. The geometrical uncertainties are from Table 1. The same procedure and line styles as for the prostate case (Fig. 5) are used except for the small bowel that is depicted instead of the bladder. Three transversal (a, b, c) and a sagittal slice (d) through the PTV are shown. The overall CTV-to-PTV margin becomes about 1 cm.

is performed, the former method will normally closely follow all irregularities in the CTV surface so all random deviations in the delineation of the CTV will be present in the PTV as well. The latter method will in itself tend to smooth the surface and can yield a slightly smaller PTV due to rounding of the corners as has been shown in Fig. 3 and Fig. 7d. Another difference will occur at small volumes or near small extensions of a volume. For volumes with diameters less than about 2 SD of the distribution of deviations, a CP value will no longer represent the probability that the volume will be partly outside of it. The actual probability will be larger. Therefore, choosing an iso-probability volume as new PTV will yield too small margins. Rigid margin addition is insensitive to the size of the input volume.

In clinical practice one might prefer a tighter CTV-to-PTV margin near a dose-limiting structure. In the model described in this paper, nearby critical organs are currently ignored in the PTV calculation. However, a critical organ might also be represented by a 3D volume matrix which can then be used to modify the CTV-to-PTV margins locally, as has been described in a previous paper about straightforward margin calculation (25). The dose probability histo-

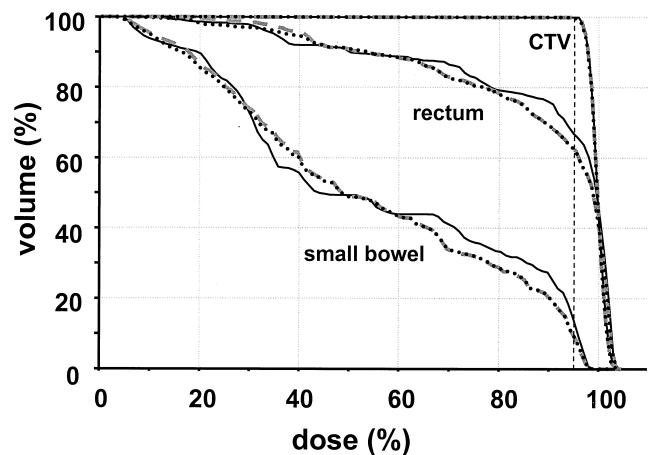


Fig. 8. Dose distribution verification for the gynecological cancer patient in Fig. 7. DVHs and DPHs for CTV, small bowel, and rectum have been calculated similar to the prostate case of Fig. 6. The effect of the random uncertainties on the rectum and small bowel (dashed gray curve) is again a significant reduction of the high dose volume compared to the original DVH (thin black curve). The DPH curves (dotted) indicate that the CTV is hardly influenced by the systematic or random deviations.



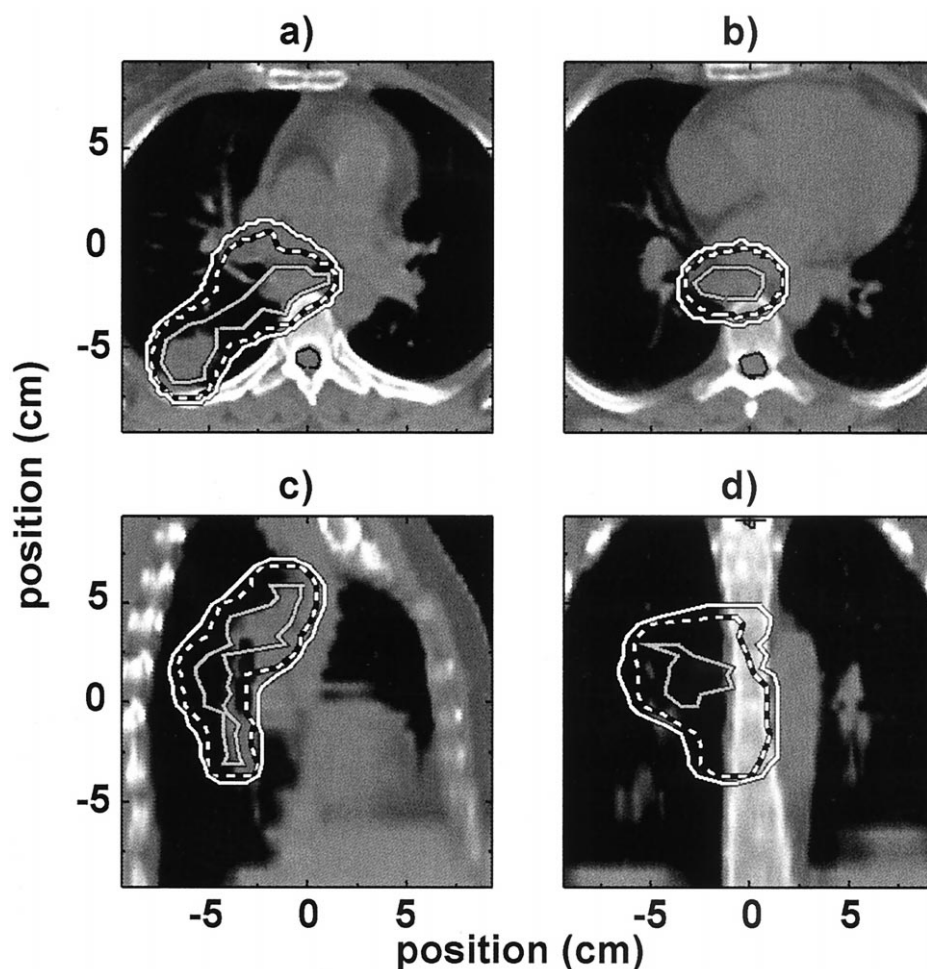


Fig. 9. Example of the PTV calculation for a lung cancer plan. The geometrical uncertainties are from Table 1. The same procedure and line styles as for the prostate case are used (Fig. 5). Two transversal (a, b), a sagittal (c), and a frontal cut (d) through the PTV are shown. The overall CTV-to-PTV margin becomes about 10–13 mm. The critical organs are the two lungs and the spinal cord.

grams can of course still be used and the influence of the local margin changes on the average dose volume histogram can immediately be visualized.

The described method assumes that all probability distributions of translations and rotations are mutually independent and of a gaussian nature. The mutual independence is however not always an accurate description of reality; for example, for internal prostate movement a relation between rotations and translations has been found (12). This might more easily be incorporated in the Monte Carlo method than in the convolution method. Instead of sampling from normal distributions, translations and rotations should be simultaneously obtained from a data base of prostate movements for a large group of patients (20). This “brute force” method will require a large data base and many samples and will therefore be time-consuming. The gaussian nature of the distributions has been verified repeatedly by studies on setup position verification. At present too few studies have been performed to establish whether this is the case for internal organ movement as well or if differently shaped

probability distributions might be more appropriate. The algorithm does however not depend on the type of probability distribution. Instead of using normal distributions for the convolutions, other distributions can be implemented as well. The output of the calculations will still be a 3D matrix with coverage probabilities which will still represent the probability that the CTV lies partly outside the corresponding voxel. Hence the same methods can be applied to obtain the PTV margins.

#### *Dose modifications*

Dose modifications that account for random deviations cause a shift of high dose to the lower dose regions. Consequently, the critical organs that receive a high dose in the original plan, like the rectum and bladder in the clinical examples, will receive less dose in the modified plan. Furthermore, from Fig. 2 is clear that the average DVH curve for systematic deviations (i.e., the DPH) can also be lower than the original, although the effect is limited for the clinical examples. This implies that the standard DVHs of



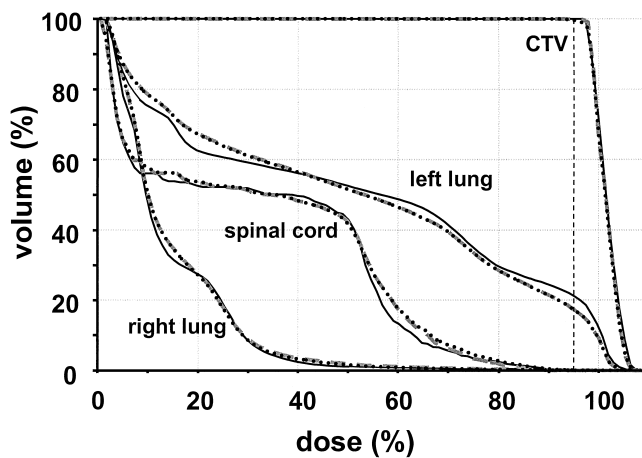


Fig. 10. DPHs and DVHs of a plan which spares the right lung for the lung cancer patient from Fig. 9. The effect of the random uncertainties (dashed gray curve) on the CTV and left lung is similar to the prostate and cervix case. However, for spinal cord and right lung the effect of random deviations is a slight increase in the high dose volume. The DPH curves (dotted) indicate that the dose distribution in the CTV is influenced by the systematic deviations but the 95% isodose is still adequately placed around the PTV.

the planning CT slightly overestimate the dose in those organs. For the critical organs that receive relatively low doses in the planning CT situation, the reverse is true. In the example for the lung cancer patient, the organs that have specially been spared (i.e., the spinal cord and the right lung) will on average receive a somewhat higher dose due to the geometrical uncertainties.

A consequence of the application running outside the planning system is that dose inhomogeneity corrections are not included when calculating the dose distribution corrected for random deviations. The effect might be less significant for calculations in the pelvic area but the accuracy of planning in the thorax or neck region will probably be affected. A further simplification of the model is that the position of the beam with respect to the direction of the deviations is of no consequence. In reality the change in dose of a volume moving in the direction of the beam is determined by the inverse square law and the slope of the depth-dose curve, which is not incorporated in the algorithm. The errors will be relatively small (26), but, ideally, dose modifications should be performed for each beam separately which would be a time-consuming procedure. In a multiple beam plan the errors are less prominent. Nonetheless, the effect of the setup deviations might be slightly overestimated.

The application can also be utilized for a check of the delivered dose after the irradiation series have been completed. Once all fractions have been delivered and portal imaging has been applied, systematic and random setup deviations can be calculated and used as input to the application to evaluate the actually delivered dose distribution. Thus it can be assessed whether the treatment has been

performed correctly and if complications or a different local control probability might be expected. The same procedure can also be applied before the end of the treatment series to verify the situation at that moment and possibly alter the course of the treatment, e.g., change the PTV margin (6). Even the actual setup deviations for every fraction might be entered separately and the consequences of the treatment on the dose can be computed more precisely.

#### *Dose probability histograms*

The concept of DPH is especially useful to determine whether the calculated dose distribution guarantees adequate CTV irradiation despite systematical uncertainties. Since the dose has been planned to conform with the CTV, every variation in CTV position will deteriorate the dose distribution in the CTV. Hence the spread in DVH curves due to systematic deviations will be reflected in the average curve. The mean DVH will therefore directly indicate the probability of CTV underdosage and hence the goodness of the plan in this respect. For critical organs however, positioning deviation in one direction might improve the DVH, movement in the opposite direction worsen the DVH, and the average will be equal to the original. Hence instead of the average DVH for all systematical deviations, the spread of the DVH curves would be more interesting (20, 21). This cannot directly be calculated using DPHs but it is possible to extend the critical organ with a margin for systematical deviations so that an indication of possible dose values in the organ is obtained. This might for instance deteriorate the lung plan because extension of the spinal cord volume might yield a significant probability of higher spinal cord dose than indicated in Fig. 10.

At first sight, there appears to be a discrepancy between Fig. 1 and the DPH calculations in this paper. Figure 1 predicts that our choice of the 2.5% iso-probability contour as PTV will for deviations in 3D result in the CTV being partly outside the PTV in at least 28% of all patients. The average DVHs (or DPHs) in the clinical examples indicate however that the probability of underdosage of the CTV (dose < 95%) is at most about a few percent. This is because the extent of CTV volume outside the PTV is small. Using a formula similar to Eq. 5, it can be calculated that the average distance that the CTV border will exceed the PTV border will be about  $0.5\sigma$  for those 28% of patients. Since clinical  $\Sigma$ -values range from about 2 to 4 mm, a 1- to 2-mm-thick slice of the CTV will be systematically outside the PTV for those patients. This is about equal to the size of one CT pixel and since the 95% isodose volume does normally not enclose the PTV exactly, the probability of underdosage is significantly smaller than the probability of the CTV being outside the PTV.

Because the tightness of the 95% isodose around the PTV will be dependent on the treatment technique used (and on the beam characteristics), the required PTV margins to guarantee a high probability of sufficient dose in the CTV despite systematical deviations will be technique-dependent

as well. For instance, for conformal techniques slightly larger PTVs are required than for conventional techniques using rectangular fields to obtain the same DPHs. The same holds for the margin for random deviations. If that margin is based on the shrinkage of the 95% isodose, this will also be technique-dependent. For patients groups with standard treatment techniques, the PTV and block margins can be optimized using the DPHs of the dose distribution modified for random deviations. Once the margins are standardized, the iteration process to obtain optimal PTV margins will be superfluous for each patient separately.

## CONCLUSION

A model has been developed which allows for the inclusion of geometrical uncertainties in the radiotherapy planning process. Required parameters are a set of 12 standard

deviations describing the various uncertainties. The model calculates PTV margins based on the requirement that on average a large part of the CTV ( $> 99\%$ ) is irradiated with a high dose ( $> 95\%$ ). The size of adequate margins appears to be approximately equal to  $2\Sigma + 0.7\sigma$ . Since rotational deviations are included, the margins can well be anisotropic. Once the patient is planned, the influence of the systematical deviations on the dose distribution in the CTV is determined by the average DVH for all systematic deviations, using so-called dose probability histograms. The influence of random deviations is determined by convolution of the dose distribution with the probability functions. In an iterative process of planning and verification of the CTV coverage, the CTV-to-PTV and block margins can be optimized for each patient separately. For standard planning techniques of specific patient groups, the margins can be standardized and the iterations omitted.

## REFERENCES

1. International Commission on Radiation Units and Measurements. ICRU Report 50: Prescribing, recording, and reporting photon beam therapy. Bethesda (MD): ICRU Publications; 1993.
2. Bel A, Vijlbrief R, Lebesque JV. Setup deviations in wedged pair irradiation of parotid gland and tonsillar tumors, measured with an electronic portal imaging device. *Radiother Oncol* 1995;37:153–159.
3. Creutzberg CL, Althof VG, de Hoog M, *et al.* A quality control study of the accuracy of patient positioning in irradiation of pelvic fields. *Int J Radiat Oncol Biol Phys* 1996;34:697–708.
4. Bel A, van Herk M, Bartelink H, *et al.* A verification procedure to improve patient set-up accuracy using portal images. *Radiother Oncol* 1993;29:253–260.
5. Bel A, Vos PH, Rodrigus PTR, *et al.* High precision prostate cancer irradiation by clinical application of an off-line patient setup verification procedure, using portal imaging. *Int J Radiat Oncol Biol Phys* 1996;35:321–332.
6. Yan D, Vicini F, Wong J, *et al.* Adaptive radiation therapy. *Phys Med Biol* 1997;42:123–132.
7. De Neve W, Van den Heuvel F, De Beukeleer M, *et al.* Routine clinical on-line portal imaging followed by immediate field adjustment using a tele-controlled patient couch. *Radiother Oncol* 1992;24:45–54.
8. Stroom J, Quint S, Seven M, *et al.* The need for on-line set-up corrections of patients with gynaecological tumors (Abstr.). *Med Phys* 1996;23:1083.
9. Balter JM, Sandler HM, Lam K, *et al.* Measurement of prostate movement over the course of routine radiotherapy using implanted markers. *Int J Radiat Oncol Biol Phys* 1995;31:113–118.
10. Crook JM, Raymond Y, Salhani D, *et al.* Prostate motion during standard radiotherapy as assessed by fiducial markers. *Radiother Oncol* 1995;37:35–42.
11. Roeske JC, Forman JD, Mesina CF, *et al.* Evaluation of changes in the size and location of the prostate, seminal vesicles, bladder, and rectum during a course of external beam RT. *Int J Radiat Oncol Biol Phys* 1995;33:1321–1329.
12. van Herk M, Bruce A, Kroes AP, *et al.* Quantification of organ motion during conformal radiotherapy of the prostate by three dimensional image registration. *Int J Radiat Oncol Biol Phys* 1995;33:1311–1320.
13. Ross CS, Hussey DH, Pennington EC, *et al.* Analysis of movement of intrathoracic neoplasms using ultrafast computerized tomography. *Int J Radiat Oncol Biol Phys* 1990;18:671–677.
14. Kubo HD, Hill BC. Respiration gated RT treatment: A technical study. *Phys Med Biol* 1996;41:83–91.
15. Morrill SM, Langer M, Lane RG. Real-time couch compensation for intra-treatment organ motion: Theoretical advantages (Abstr.). *Med Phys* 1996;23:1083.
16. Wong JW, Sharpe MB, Jaffray DA. Minimizing intra-fraction organ motion with active breathing control (Abstr.) *Med Phys* 1997;24:1022.
17. Hunt MA, Shultheiss TE, Desoobry G, *et al.* Convolving set-up uncertainties with dose distributions (Abstr.). *Med Phys* 1993;20:929.
18. Rudat V, Flentje M, Oetzel D, *et al.* Influence of the positioning error on 3D conformal dose distributions during fractionated radiotherapy. *Radiother Oncol* 1994;33:56–63.
19. Goitein M. Calculation of the uncertainty in the dose delivered during radiation therapy. *Med Phys* 1985;12:608–612.
20. Mageras GS, Kutcher GJ, Leibel SA, *et al.* A method of incorporating organ motion uncertainties into three-dimensional treatment plans. *Int J Radiat Oncol Biol Phys* 1996;35:333–342.
21. Killoran JH, Kooy HM, Gladstone DJ, *et al.* A numerical simulation of organ motion and daily setup uncertainties: Implications for radiation therapy. *Int J Radiat Oncol Biol Phys* 1997;37:213–221.
22. Stroom JC, Korevaar GA, Koper PC, *et al.* Multiple two-dimensional versus three-dimensional PTV definition in treatment planning for conformal radiotherapy. *Radiother Oncol* 1998;47:297–302.
23. Austin-Seymour M, Kalet I, McDonald J, *et al.* Three dimensional planning target volumes: A model and a software tool. *Int J Radiat Oncol Biol Phys* 1995;33:1073–1080.
24. Belshi R, Pontvert D, Rosenwald JC, *et al.* Automatic three-dimensional expansion of structures applied to determination of the clinical target volume in conformal radiotherapy. *Int J Radiat Oncol Biol Phys* 1997;37:689–696.
25. Stroom JC, Storchi PRM. Automatic calculation of three-dimensional margins around treatment volumes in radiotherapy planning. *Phys Med Biol* 1997;42:745–755.

26. Bel A, van Herk M, Lebesque JV. Target margins for random geometrical treatment uncertainties in conformal radiotherapy. *Med Phys* 1996;23:1537–1547.
27. Stroom JC, Visser AG, de Boer JCJ, *et al.* Use of coverage probability to quantify results of clinical positioning studies in radiotherapy planning. In: Hounsell AR, Wilkinson JM, Williams PC, editors. *Proceedings of the XIth International Conference on the Use of Computers in Radiation Therapy*. Manchester: North Western Medical Physics Department, Christie Hospital; 1994. p.264–265.